Supporting Information for: Large Scale Electronic Correlation Calculations: Rank-Reduced Full Configuration Interaction

B. Scott Fales,[†,‡] Stefan Seritan,[†,‡] Nick F. Settje,[†,‡] Benjamin G. Levine,[¶] Henrik Koch,[§] and Todd J. Martínez[*,†,‡]

†*Department of Chemistry and the PULSE Institute, Stanford University, Stanford, CA 94305, United States*

‡*SLAC National Accelerator Laboratory, Menlo Park, California 94025, United States*

¶*Department of Chemistry, Michigan State University, East Lansing, MI 48824*

§*Department of Chemistry, Norwegian University of Science and Technology, 7491 Trondheim, Norway*

E-mail: toddjmartinez@gmail.com

1 Naphthalene and Anthracene Wavefunction $\langle S^2 \rangle$

While the ansatz $\mathbf{\Psi_i} = \mathbf{P^i} \otimes \mathbf{Q^i} \pm \mathbf{Q^i} \otimes \mathbf{P^i}$ eliminates singlet/triplet spin contamination, higher angular momentum contamination may still occur. To evaluate the extent to which this contamination is present in the RR-FCI wavefunction we have determined $\langle S^2 \rangle$ for each contributing product term as well as for the whole wavefunction as each product term is added. This methodology was applied to both the singlet and triplet states of Naphthalene and Anthracene, the results of which are provided in Figures S1 — S4.

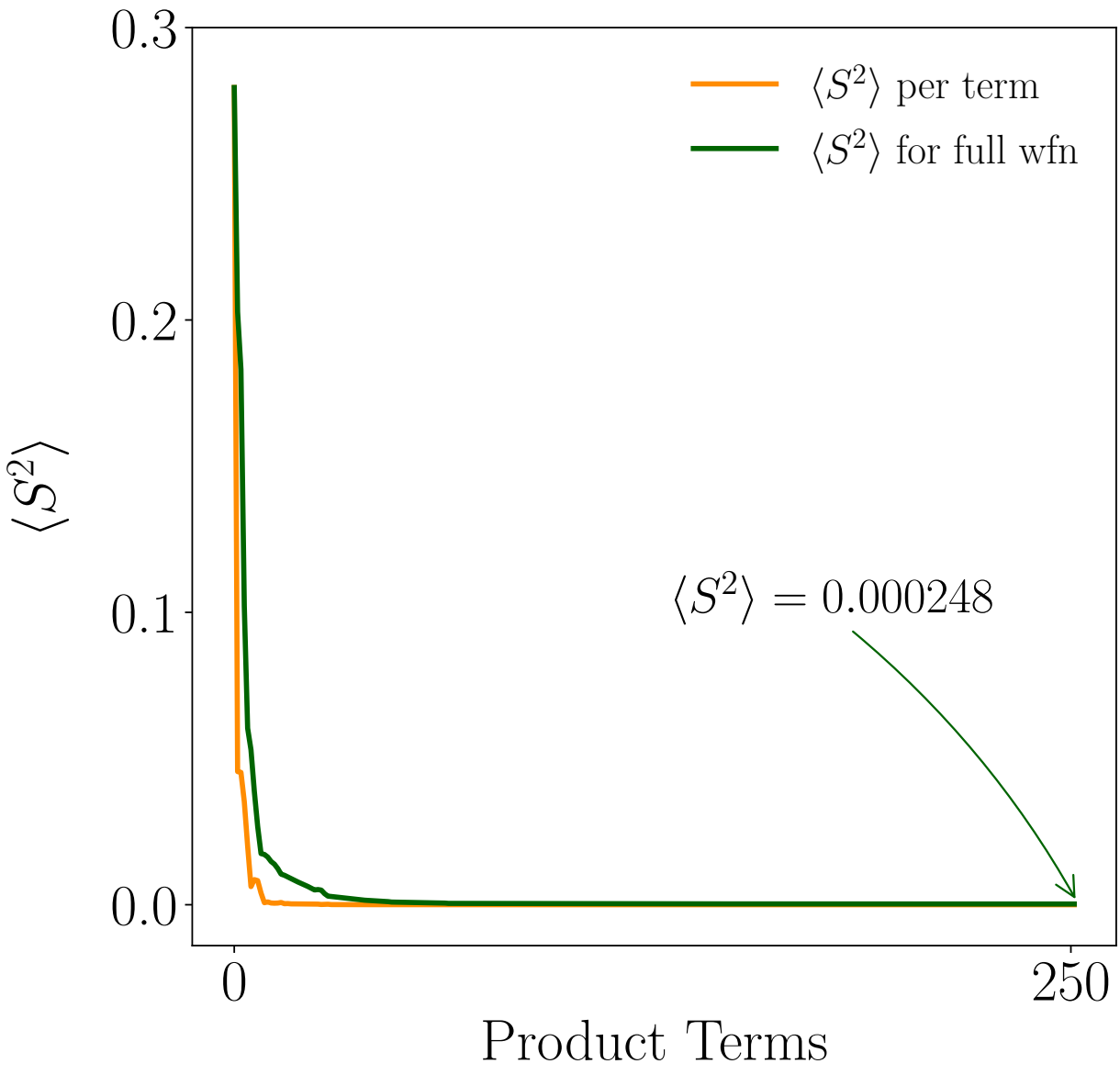

Figure S1: $\langle S^2 \rangle$ for the ground singlet state of Napthalene at RR-CAS-(10,10)-CI/cc-pVDZ. Values for each product term and for the current total wavefunction $\mathbf{\Psi}$ are depicted in orange and green, respectively. The spin expectation of the final wavefunction after 252 product terms were added is 0.000248.

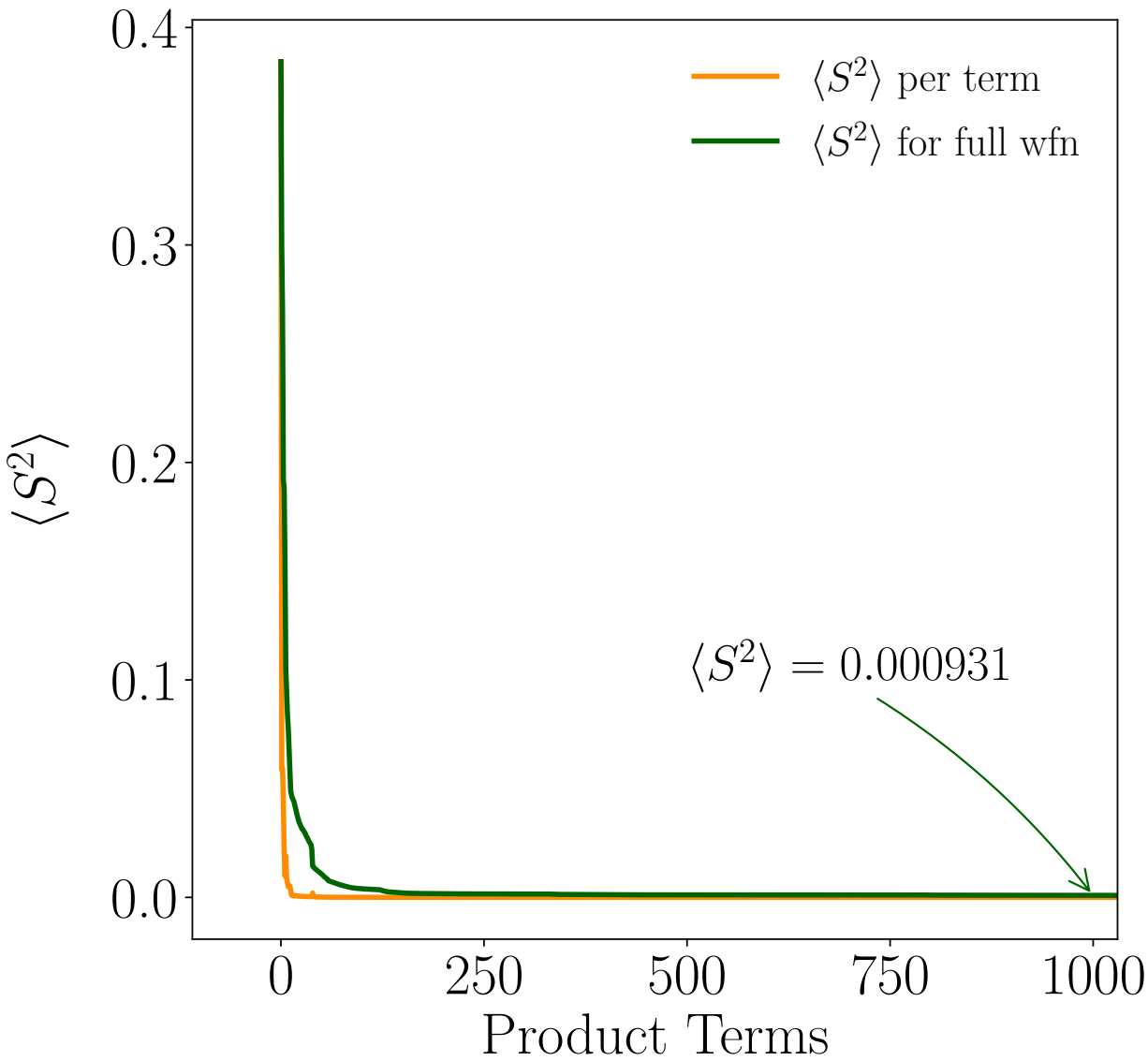

Figure S2: $\langle S^2 \rangle$ for the ground singlet state of Anthracene at RR-CAS-(14,14)-CI/cc-pVDZ. Values for each product term and for the current total wavefunction $\mathbf{\Psi}$ are depicted in orange and green, respectively. The spin expectation of the final wavefunction after 1000 product terms were added is 0.000931.

Each of the singlet Naphthalene and Anthracene wavefunctions contain spin contamination when only a few product terms are present, but subsequent addition of only a few dozen terms quickly brings the contamination to within 0.01 of the spin-pure state. In both cases spin purity of $< 10^{-3}$ was achieved with the final converged wavefunction.

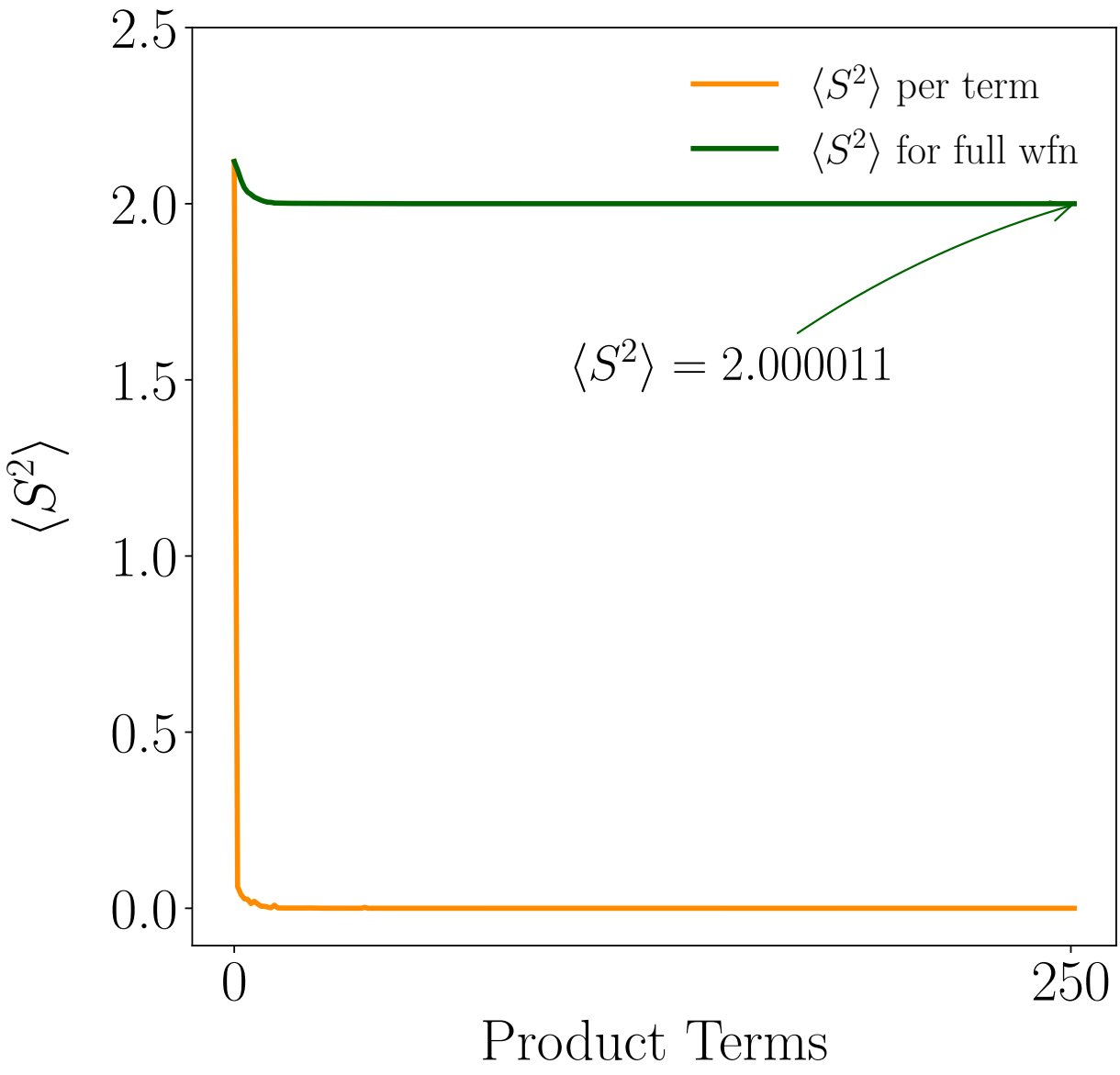

Figure S3: $\langle S^2 \rangle$ for the ground triplet state of Naphthalene at RR-CAS-(10,10)-CI/cc-pVDZ. Values for each product term and for the current total wavefunction $\mathbf{\Psi}$ are depicted in orange and green, respectively. The spin expectation of the final wavefunction after 252 product terms were added is 2.000011.

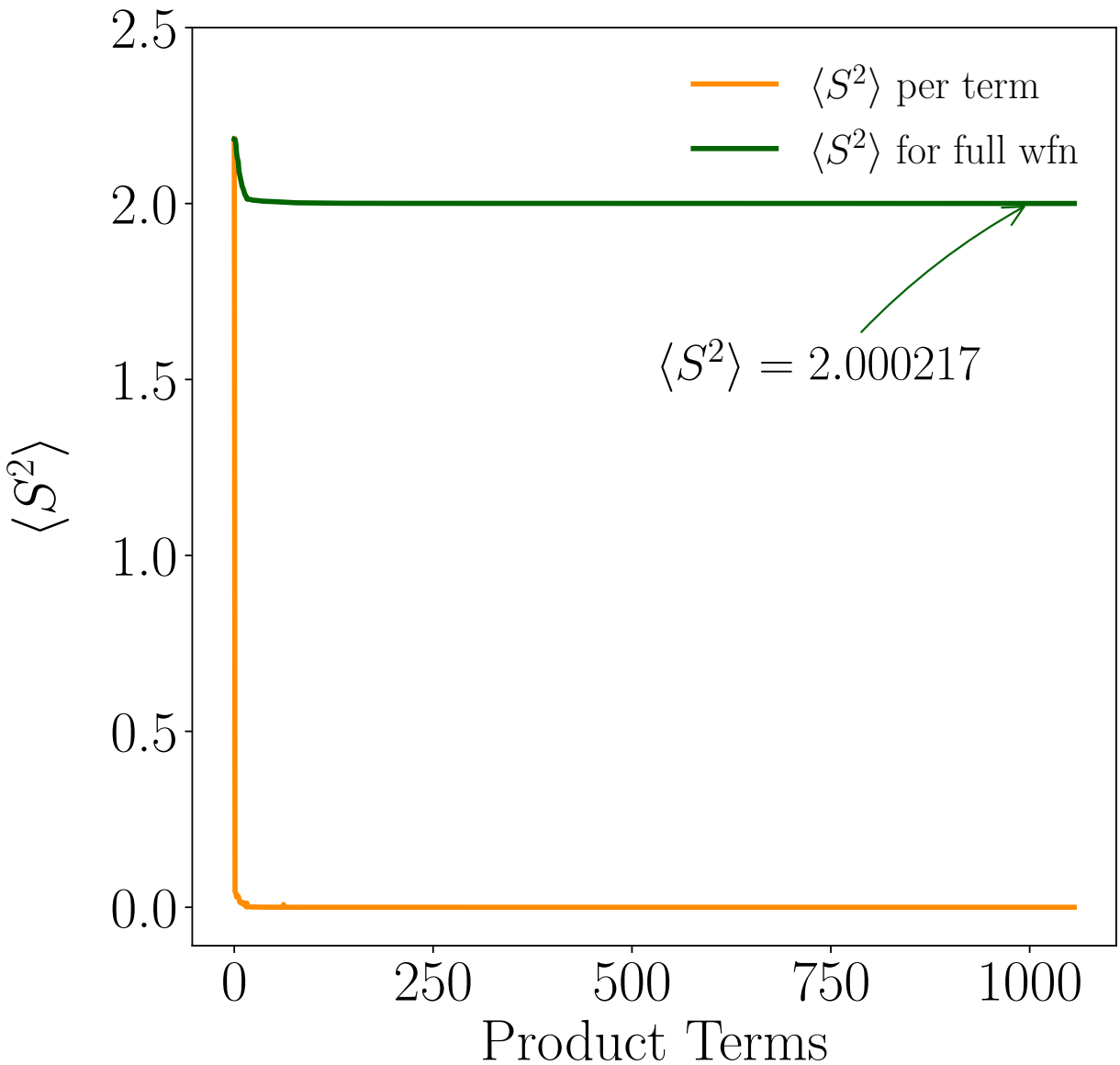

Figure S4: $\langle S^2 \rangle$ for the ground triplet state of Anthracene at RR-CAS-(14,14)-CI/cc-pVDZ. Values for each product term and for the current total wavefunction $\mathbf{\Psi}$ are depicted in orange and green, respectively. The spin expectation of the final wavefunction after 1000 product terms were added is 2.000217.

Triplet calculations for Naphthalene and Anthracene behave similarly as their singlet counterparts, except that the $\langle S^2 \rangle$ of each product term after the first has significant singlet character. These additional product terms serve both to refine the energy and to purify the spin components of the wavefunction. The triplet wavefunctions become more spin pure with fewer product terms relative to the singlet wavefunctions for the same systems, and the

contamination of the final wavefunctions for Naphthalene and Anthracene is less than 10^{-4} and 10^{-3}, respectively.

2 Alternative Projected $\boldsymbol{\sigma}$ Algorithm

Projected $\boldsymbol{\sigma}$ formation is defined as

$$\boldsymbol{\sigma}^{\mathbf{P}}_{J'} = \sum_{J,K,K'}^{N_{str}} Q_{K'} \langle \phi^{\alpha}_{J'}, \phi^{\beta}_{K'} | \hat{H} | \phi^{\alpha}_{J}, \phi^{\beta}_{K} \rangle P_J Q_K \tag{1}$$

for projection onto the $\mathbf{P}$ space while projection onto the $\mathbf{Q}$ vector space gives

$$\boldsymbol{\sigma}^{\mathbf{Q}}_{K'} = \sum_{J,J',K}^{N_{str}} P_{J'} \langle \phi^{\alpha}_{J'}, \phi^{\beta}_{K'} | \hat{H} | \phi^{\alpha}_{J}, \phi^{\beta}_{K} \rangle P_J Q_K \tag{2}$$

Algorithms $1-3$ describe $\mathbf{P}$ vector optimization projected $\boldsymbol{\sigma}$ formation using an orbital label driven method analogous to the CI approach described by Olsen.

Algorithm 1 Factorized $\boldsymbol{\sigma_1}$ formation algorithm.

```
Q = ±(Q_l · Q_r)
for k, l < N_o do
    F ← 0.0                                          ▷ Work array of size N_str
    for I < N_str do
        M ← ij_to_I[k, l, I]
        I' ← ij_to_J[k, l, I]
        F[M] ← γ[k][l] * P_r[I']
    end for
    σ += Q * h'_kl[k][l] * F                         ▷ (DAXPY)
    for i, j < N_o do
        for I < N_str do
            M ← ij_to_I[k, l, I]
            I' ← ij_to_J[k, l, I]
            σ[I'] += 0.5 * Q * γ[i][j] * (ij|kl) * F[M]
        end for
    end for
end for
```

Algorithm 2 Factorized $\boldsymbol{\sigma_2}$ formation algorithm.

```
for k, l < N_o do
    F ← 0.0                                          ▷ Work array of size N_str
    for I < N_str do
        M ← ij_to_I[k, l, I]
        I' ← ij_to_J[k, l, I]
        F[M] ← γ[k][l] * Q_r[I']
    end for
    s += h'_kl[k][l] * F                             ▷ (DAXPY)
    for i, j < N_o do
        for I < N_str do
            M ← ij_to_I[k, l, I]
            I' ← ij_to_J[k, l, I]
            s[I'] += 0.5 * γ[i][j] * (ij|kl) * F[M]
        end for
    end for
end for
PQ = ±(P_r · s)
σ += PQ * Q_l                                        ▷ (DAXPY)
```

Algorithm 3 Factorized $\boldsymbol{\sigma_3}$ formation algorithm.

```
for k, l < N_o do
    F ← 0.0                                          ▷ Work array of size N_str
    for I < N_str do
        M ← ij_to_I[k, l, I]
        I' ← ij_to_J[k, l, I]
        F[M] ← γ[k][l] * Q_r[I']
    end for
    PQ = ±(P_r · F)
    for i, j < N_o do
        for I < N_str do
            M ← ij_to_I[k, l, I]
            I' ← ij_to_J[k, l, I]
            σ[M] += 0.5 * PQ * γ[i][j] * (ij|kl) * Q_l[I']
        end for
    end for
end for
```

The $\mathbf{Q_l}$, $\mathbf{Q_r}$, and $\mathbf{P_r}$ correspond to the left $\mathbf{Q}$ vector, the right $\mathbf{Q}$ vector, and the $\mathbf{P}$ vector in Equation 1. Each of the $\mathbf{PQ}^T$ and the $\mathbf{QP}^T$ term projected $\boldsymbol{\sigma}$ can be formed (for both $\mathbf{P}$ and $\mathbf{Q}$ vector optimizations) using these algorithms and interchanging the ordering and identities of the input vectors. In the above algorithms the $\boldsymbol{\gamma}$ are indexed by the orbital labels i, j, and the **ij_to_I** and **ij_to_J** matrices map orbital indices ij to the configuration string labels M and I'.

Vectorized algorithms require contiguous access of data structures to avoid performance penalties. For example, in Algorithm 1, elements of the $\boldsymbol{\gamma}$ matrix are accessed contiguously, and even though both the $\mathbf{P_r}$ and $\boldsymbol{\sigma}$ vectors are accessed randomly, gathering of the $\mathbf{P_r}$ elements into the $\mathbf{F}$ matrix allows the higher scaling contraction with the two-electron integrals $(\mathbf{ij}|\mathbf{kl})$ to be performed using coalesced memory access patterns. Gather-scatter techniques are also used in Algorithm 2 to reduce memory pressure. The highest scaling operation in $\boldsymbol{\sigma_3}$ formation does not benefit from contiguous memory access, however, where the $(\mathbf{ij}|\mathbf{kl})$ are contracted directly with the $\mathbf{Q_l}$ vector (Algorithm 3). Efforts to improve access patterns here do not translate well to GPU hardware, where repeated manipulation of arrays must be performed to avoid strided memory access.

3 Tiled and Unrolled $\boldsymbol{\sigma}^{\boldsymbol{P}}$ Algorithm

The projected $\boldsymbol{\sigma}$ formation corresponding to the eigenvalue equation component

$$\sum_{J,K,K'}^{N_{str}} \left[\langle (\phi_{J'}^{\alpha}, Q_{K'}) \pm (Q_{K'}, \phi_{J'}^{\beta}) | \hat{H} - E | (\phi_{J}^{\alpha}, Q_{K}) \pm (Q_{K}, \phi_{J}^{\beta}) \rangle \right] P_J = 0 \tag{3}$$

is the rate-limiting step of the RR-FCI iterations. Incorporating ideas from the work of Knowles and Handy[1] we can improve upon the approaches described in Algorithms 1–3. The following algorithms (4–6) describe in detail our methods for obtaining the projected $\boldsymbol{\sigma}$ vectors.

Algorithm 4 GPU vectorized projected $\boldsymbol{\sigma_1}$ algorithm. $\mathbf{l}$ are orbital indices given a string pair I, I', and $\mathbf{D}$ and $\mathbf{E}$ are floating point arrays.

```
Q = 2 * Q · Q                                                          ▷ DDOT
for B < N_blocks do
    D ← 0.0                                                            ▷ memset
    GPU vectorize over strings I in block B, all I' differing from I by one occupation
        ij ← l[I][I']
        D[ij, I] += γ[α][I']P[I']
    end GPU vectorize
    GPU vectorize over strings I in block B
        ij ← l[I][I]
        D[ij, I] += P[I]
    end GPU vectorize
    σ += Q * D * h'_kl                                                 ▷ DGEMV
    E ← 0.5 * Q * (ij|kl) * D                                          ▷ DGEMM
    GPU vectorize over strings I in block B, all I' differing from I one occupation
        ij ← l[I][I']
        σ[I'] += γ[I][I']E[ij, I]                                      ▷ Atomic operation
    end GPU vectorize
    GPU vectorize over strings I in block B
        ij ← l[I][I]
        σ[I] += E[ij, I]                                               ▷ Atomic operation
    end GPU vectorize
end for
Q = ± 2 * P · Q                                                        ▷ DDOT
for B < N_blocks do
    D ← 0.0                                                            ▷ memset
    GPU vectorize over strings I in block B, all I' differing from I by one occupation
        ij ← l[I][I']
        D[ij, I] += γ[I][I']Q[I']
    end GPU vectorize
    GPU vectorize over strings I in block B
        ij ← l[I][I]
        D[ij, I] += Q[I]
    end GPU vectorize
    σ += Q * D * h'_kl                                                 ▷ DGEMV
    E ← 0.5 * Q * (ij|kl) * D                                          ▷ DGEMM
    GPU vectorize over strings I in block B, all I' differing from I one occupation
        ij ← l[I][I']
        σ[I'] += γ[I][I']E[ij, I]                                      ▷ Atomic operation
    end GPU vectorize
    GPU vectorize over strings I in block B
        ij ← l[I][I]
        σ[I] += E[ij, I]                                               ▷ Atomic operation
    end GPU vectorize
end for
```

Algorithm 5 GPU vectorized projected $\boldsymbol{\sigma_2}$ algorithm. $\mathbf{l}$ are orbital indices given a string pair I, I', $\mathbf{s}$ is an array that accumulates the temporary $\boldsymbol{\sigma}$ vector, and $\mathbf{D}$ and $\mathbf{E}$ are floating point arrays.

```
for B < N_blocks do
    D ← 0.0                                                          ▷ memset
    GPU vectorize over strings I in block B, all I' differing from I by one occupation
        ij ← l[I][I']
        D[ij, I] += γ[I][I'] Q[I']
    end GPU vectorize
    GPU vectorize over strings I in block B
        ij ← l[I][I]
        D[ij, I] += Q[I]
    end GPU vectorize
    s += D * h'_kl                                                   ▷ DGEMV
    E ← 0.5 * (ij|kl) * D                                            ▷ DGEMM
    GPU vectorize over strings I in block B, all I' differing from I by one occupation
        ij ← l[I][I']
        s[I'] += γ[I][I'] E[ij, I]                                   ▷ Atomic operation
    end GPU vectorize
    GPU vectorize over strings I in block B
        ij ← l[I][I]
        s[I'] += E[ij, I]                                            ▷ Atomic operation
    end GPU vectorize
end for
PQ = ± 2 * P · s                                                     ▷ DDOT
σ += PQ * Q                                                          ▷ DAXPY
PQ = 2 * Q · s                                                       ▷ DDOT
σ += PQ * P                                                          ▷ DAXPY
```

Algorithm 6 GPU vectorized projected $\boldsymbol{\sigma_3}$ algorithm. $\mathbf{l}$ are orbital indices given a string pair I, I', $\mathbf{s}$ is an array that accumulates the temporary $\boldsymbol{\sigma}$ vector, and $\mathbf{D}$ and $\mathbf{E}$ are floating point arrays.

```
for B < N_blocks do
    D ← 0.0                                                          ▷ memset
    GPU vectorize over strings I in block B, I' differing from I by one occupation
        ij ← l[I][I']
        D[ij, I] += γ[I][I']Q[I']
    end GPU vectorize
    GPU vectorize over strings I in block B
        ij ← l[I][I]
        D[ij, I] += Q[I]
    end GPU vectorize
    s ← D * P                                                        ▷ DGEMV
    E ← (ij|kl) * D                                                  ▷ DGEMM
    σ ±= 2 * E * s                                                   ▷ DGEMV
    D ← 0.0                                                          ▷ memset
    GPU vectorize over strings I in block B, I' differing from I by one occupation
        ij ← l[I][I']
        D[ij, I] += γ[I][I']Q[I']
    end GPU vectorize
    GPU vectorize over strings I in block B
        ij ← l[I][I]
        D[ij, I] += Q[I]
    end GPU vectorize
    s ← D * Q                                                        ▷ DGEMV
    D ← 0.0                                                          ▷ memset
    GPU vectorize over strings I in block B, I' differing from I by one occupation
        ij ← l[I][I']
        D[ij, I] += γ[I][I']P[I']
    end GPU vectorize
    GPU vectorize over strings I in block B
        ij ← l[I][I]
        D[ij, I] += P[I]
    end GPU vectorize
    E ← (ij|kl) * D                                                  ▷ DGEMM
    σ += 2 * E * s                                                   ▷ DGEMV
end for
```

4 Supporting Geometries

We provide Cartesian coordinates for the ethylene dimer and acene structures used in this work in units of Angstrom (Å).

Ethylene Dimer ($C_2H_4)_2$

	X	Y	Z
C	0.35673483	-0.05087227	-0.47786734
C	1.61445821	-0.06684947	-0.02916681
H	-0.14997206	0.87780529	-0.62680155
H	-0.16786485	-0.95561368	-0.69426370
H	2.15270896	0.84221076	0.19314809
H	2.16553127	-0.97886933	0.15232587
C	6.35673483	-0.05087227	-0.47786734
C	7.61445821	-0.06684947	-0.02916681
H	5.85000000	0.87780529	-0.62680155
H	5.84000000	-0.95561368	-0.69426370
H	8.15270896	0.84221076	0.19314809
H	8.16553127	-0.97886933	0.15232587

Singlet Naphthalene ($C_{10}H_8$)

	X	Y	Z
C	-2.433661	0.708302	0.000000
C	-2.433661	-0.708302	0.000000
H	-3.378045	-1.245972	0.000000
H	-3.378045	1.245972	0.000000
C	-1.244629	1.402481	0.000000
C	-1.244629	-1.402481	0.000000
C	-0.000077	0.717168	0.000000
C	-0.000077	-0.717168	0.000000
H	-1.242734	2.490258	0.000000
H	-1.242734	-2.490258	0.000000
C	1.244779	1.402533	0.000000
C	1.244779	-1.402533	0.000000
C	2.433606	0.708405	0.000000
C	2.433606	-0.708405	0.000000
H	1.242448	2.490302	0.000000
H	1.242448	-2.490302	0.000000
H	3.378224	1.245662	0.000000
H	3.378224	-1.245662	0.000000

Triplet Naphthalene ($C_{10}H_8$)

	X	Y	Z
C	2.488282	0.681831	0.000000
C	2.488282	-0.681831	0.000000
H	3.419575	-1.241120	0.000000
H	3.419575	1.241120	0.000000
C	1.238411	1.400670	0.000000
C	1.238411	-1.400670	0.000000
C	-0.000001	0.725296	0.000000
C	-0.000001	-0.725296	0.000000
H	1.247313	2.487396	0.000000
H	1.247313	-2.487396	0.000000
C	-1.238411	1.400665	0.000000
C	-1.238411	-1.400665	0.000000
C	-2.488281	0.681833	0.000000
C	-2.488281	-0.681833	0.000000
H	-1.247325	2.487390	0.000000
H	-1.247325	-2.487390	0.000000
H	-3.419563	1.241141	0.000000
H	-3.419563	-1.241141	0.000000

Singlet Anthracene ($C_{14}H_{10}$)

	X	Y	Z
C	-3.660857	0.713070	0.000000
C	-3.660857	-0.713070	0.000000
H	-4.607652	-1.246404	0.000000
H	-4.607652	1.246404	0.000000
C	-2.479632	1.407088	0.000000
C	-2.479632	-1.407088	0.000000
C	-1.224085	0.722636	0.000000
C	-1.224085	-0.722636	0.000000
H	-2.477321	2.494657	0.000000
H	-2.477321	-2.494657	0.000000
C	0.000029	1.403284	0.000000
C	0.000029	-1.403284	0.000000
C	1.224035	0.722646	0.000000
C	1.224035	-0.722646	0.000000
H	-0.000033	2.491609	0.000000
H	-0.000033	-2.491609	0.000000
C	2.479679	1.407102	0.000000
C	2.479679	-1.407102	0.000000
C	3.660841	0.713104	0.000000
C	3.660841	-0.713104	0.000000
H	2.477242	2.494663	0.000000
H	2.477242	-2.494663	0.000000
H	4.607703	1.246313	0.000000
H	4.607703	-1.246313	0.000000

Triplet Anthracene ($C_{14}H_{10}$)

	X	Y	Z
C	3.706046	0.691777	0.000000
C	3.706046	-0.691777	0.000000
H	4.641764	-1.243830	0.000000
H	4.641764	1.243830	0.000000
C	2.480846	1.395697	0.000000
C	2.480846	-1.395697	0.000000
C	1.255174	0.720576	0.000000
C	1.255174	-0.720576	0.000000
H	2.484966	2.483134	0.000000
H	2.484966	-2.483134	0.000000
C	0.000000	1.406192	0.000000
C	0.000000	-1.406192	0.000000
C	-1.255173	0.720575	0.000000
C	-1.255173	-0.720575	0.000000
H	-0.000001	2.493700	0.000000
H	-0.000001	-2.493700	0.000000
C	-2.480846	1.395696	0.000000
C	-2.480846	-1.395696	0.000000
C	-3.706045	0.691777	0.000000
C	-3.706045	-0.691777	0.000000
H	-2.484968	2.483133	0.000000
H	-2.484968	-2.483133	0.000000
H	-4.641762	1.243835	0.000000
H	-4.641762	-1.243835	0.000000

Singlet Tetracene ($C_{18}H_{12}$)

	X	Y	Z
C	4.889184	0.715267	0.000000
C	4.889184	-0.715267	0.000000
H	5.837094	-1.246479	0.000000
H	5.837094	1.246479	0.000000
C	3.711380	1.409387	0.000000
C	3.711380	-1.409387	0.000000
C	2.450840	0.725941	0.000000
C	2.450840	-0.725941	0.000000
H	3.709630	2.496931	0.000000
H	3.709630	-2.496931	0.000000
C	1.235427	1.406152	0.000000
C	1.235427	-1.406152	0.000000
C	0.000016	0.726124	0.000000
C	0.000016	-0.726124	0.000000
H	1.235305	2.494321	0.000000
H	1.235305	-2.494321	0.000000
C	-1.235526	1.406147	0.000000
C	-1.235526	-1.406147	0.000000
C	-2.450799	0.725948	0.000000
C	-2.450799	-0.725948	0.000000
H	-1.235335	2.494309	0.000000
H	-1.235335	-2.494309	0.000000
C	-3.711407	1.409399	0.000000
C	-3.711407	-1.409399	0.000000
C	-4.889136	0.715307	0.000000
C	-4.889136	-0.715307	0.000000
H	-3.709510	2.496929	0.000000
H	-3.709510	-2.496929	0.000000
H	-5.837057	1.246476	0.000000
H	-5.837057	-1.246476	0.000000

Triplet Tetracene ($C_{18}H_{12}$)

	X	Y	Z
C	-4.926099	0.698684	0.000000
C	-4.926099	-0.698684	0.000000
H	-5.865246	-1.244975	0.000000
H	-5.865246	1.244975	0.000000
C	-3.716632	1.397315	0.000000
C	-3.716632	-1.397315	0.000000
C	-2.486849	0.717519	0.000000
C	-2.486849	-0.717519	0.000000
H	-3.717388	2.484893	0.000000
H	-3.717388	-2.484893	0.000000
C	-1.231329	1.404734	0.000000
C	-1.231329	-1.404734	0.000000
C	0.000000	0.730940	0.000000
C	0.000000	-0.730940	0.000000
H	-1.236114	2.492628	0.000000
H	-1.236114	-2.492628	0.000000
C	1.231329	1.404734	0.000000
C	1.231329	-1.404734	0.000000
C	2.486848	0.717519	0.000000
C	2.486848	-0.717519	0.000000
H	1.236114	2.492628	0.000000
H	1.236114	-2.492628	0.000000
C	3.716633	1.397314	0.000000
C	3.716633	-1.397314	0.000000
C	4.926099	0.698684	0.000000
C	4.926099	-0.698684	0.000000
H	3.717391	2.484892	0.000000
H	3.717391	-2.484892	0.000000
H	5.865245	1.244978	0.000000
H	5.865245	-1.244978	0.000000

Singlet Pentacene ($C_{22}H_{14}$)

	X	Y	Z
C	6.117721	0.716456	0.000000
C	6.117721	-0.716456	0.000000
H	7.065952	-1.247064	0.000000
H	7.065952	1.247064	0.000000
C	4.941657	1.410527	0.000000
C	4.941657	-1.410527	0.000000
C	3.678746	0.727647	0.000000
C	3.678746	-0.727647	0.000000
H	4.939919	2.498020	0.000000
H	4.939919	-2.498020	0.000000
C	2.467582	1.407836	0.000000
C	2.467582	-1.407836	0.000000
C	1.226500	0.728534	0.000000
C	1.226500	-0.728534	0.000000
H	2.467624	2.495998	0.000000
H	2.467624	-2.495998	0.000000
C	-0.000028	1.408524	0.000000
C	-0.000028	-1.408524	0.000000
C	-1.226469	0.728539	0.000000
C	-1.226469	-0.728539	0.000000
H	-0.000017	2.496573	0.000000
H	-0.000017	-2.496573	0.000000
C	-2.467625	1.407846	0.000000
C	-2.467625	-1.407846	0.000000
C	-3.678713	0.727655	0.000000
C	-3.678713	-0.727655	0.000000
H	-2.467643	2.496006	0.000000
H	-2.467643	-2.496006	0.000000
C	-4.941671	1.410535	0.000000
C	-4.941671	-1.410535	0.000000
C	-6.117708	0.716482	0.000000
C	-6.117708	-0.716482	0.000000
H	-4.939849	2.498024	0.000000
H	-4.939849	-2.498024	0.000000
H	-7.065930	1.247100	0.000000
H	-7.065930	-1.247100	0.000000

Triplet Pentacene ($C_{22}H_{14}$)

	X	Y	Z
C	-6.148662	0.703577	0.000000
C	-6.148662	-0.703577	0.000000
H	-7.090330	-1.245586	0.000000
H	-7.090330	1.245586	0.000000
C	-4.949456	1.399985	0.000000
C	-4.949456	-1.399985	0.000000
C	-3.712886	0.717632	0.000000
C	-3.712886	-0.717632	0.000000
H	-4.948444	2.487564	0.000000
H	-4.948444	-2.487564	0.000000
C	-2.464142	1.403071	0.000000
C	-2.464142	-1.403071	0.000000
C	-1.244230	0.729785	0.000000
C	-1.244230	-0.729785	0.000000
H	-2.468456	2.491214	0.000000
H	-2.468456	-2.491214	0.000000
C	0.000000	1.408308	0.000000
C	0.000000	-1.408308	0.000000
C	1.244230	0.729785	0.000000
C	1.244230	-0.729785	0.000000
H	0.000000	2.496125	0.000000
H	0.000000	-2.496125	0.000000
C	2.464142	1.403071	0.000000
C	2.464142	-1.403071	0.000000
C	3.712886	0.717632	0.000000
C	3.712886	-0.717632	0.000000
H	2.468456	2.491214	0.000000
H	2.468456	-2.491214	0.000000
C	4.949456	1.399985	0.000000
C	4.949456	-1.399985	0.000000
C	6.148662	0.703577	0.000000
C	6.148662	-0.703577	0.000000
H	4.948445	2.487564	0.000000
H	4.948445	-2.487564	0.000000
H	7.090329	1.245586	0.000000
H	7.090329	-1.245586	0.000000

References

(1) Knowles, P. J.; Handy, N. C. A New Determinant Based Full Configuration Interaction Method. *Chem. Phys. Lett.* **1984**, *111*, 315–321.